

Electronic Supplementary Information for

Electrochemical and Electronic Properties of LiCoO₂
Cathode Investigated by Galvanostatic Cycling and
EIS[†]

Xiang-Yun Qiu^{ab}, Quan-Chao Zhuang^{*a}, Qian-Qian Zhang^a, Ru Cao^a, Peng-Zhan
Ying^b, Ying-Huai Qiang^a, Shi-Gang Sun^{*c}

^a *Li-ion Batteries Lab, School of Materials Science and Engineering, China University of Mining and Technology, Xuzhou 221116, China;*

^b *School of Chemical Engineering and Technology, China University of Mining and Technology, Xuzhou 221116, China;*

^c *State Key Lab of Physical Chemistry of Solid Surfaces, Department of Chemistry, College of Chemistry and Chemical Engineering, Xiamen University, Xiamen 361005, China.*

*Corresponding author: E-mail: zhuangquanchao@126.com, sgsun@xmu.edu.cn

This file includes some results for Nyquist plots of the blank electrode without LiCoO₂, and the LiCoO₂ electrode in the two-electrode button cell during the first delithiation/lithiation process and after the 10th cycle; Variations of R_{SEI} , R_e , R_{ct} , capacitance values with electrode potential obtained from fitting the experimental impedance spectra, including Fig. S1-S8.

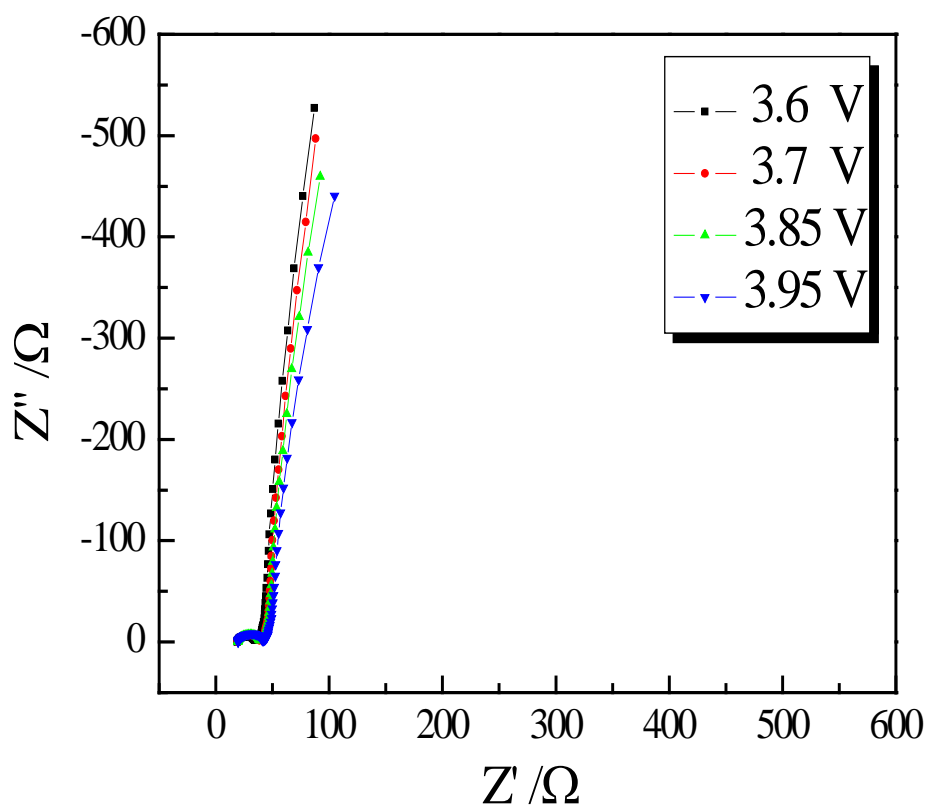


Fig. S1 Nyquist plots of the blank electrode (carbon black and graphite without LiCoO_2) at the significant potentials 3.6, 3.7, 3.85 and 3.95 V.

Note: The feature of Nyquist plots of the blank electrode without LiCoO_2 are similar without significant change besides the HFS increasing slowly with the increase of electrode polarization potential, indicating the blank electrode has a quite different feature from the LiCoO_2 electrode in the EIS test. This means that the conductive additive (carbon black and graphite) does not affect the attribution of the three semicircles in the EIS of the LiCoO_2 electrode.

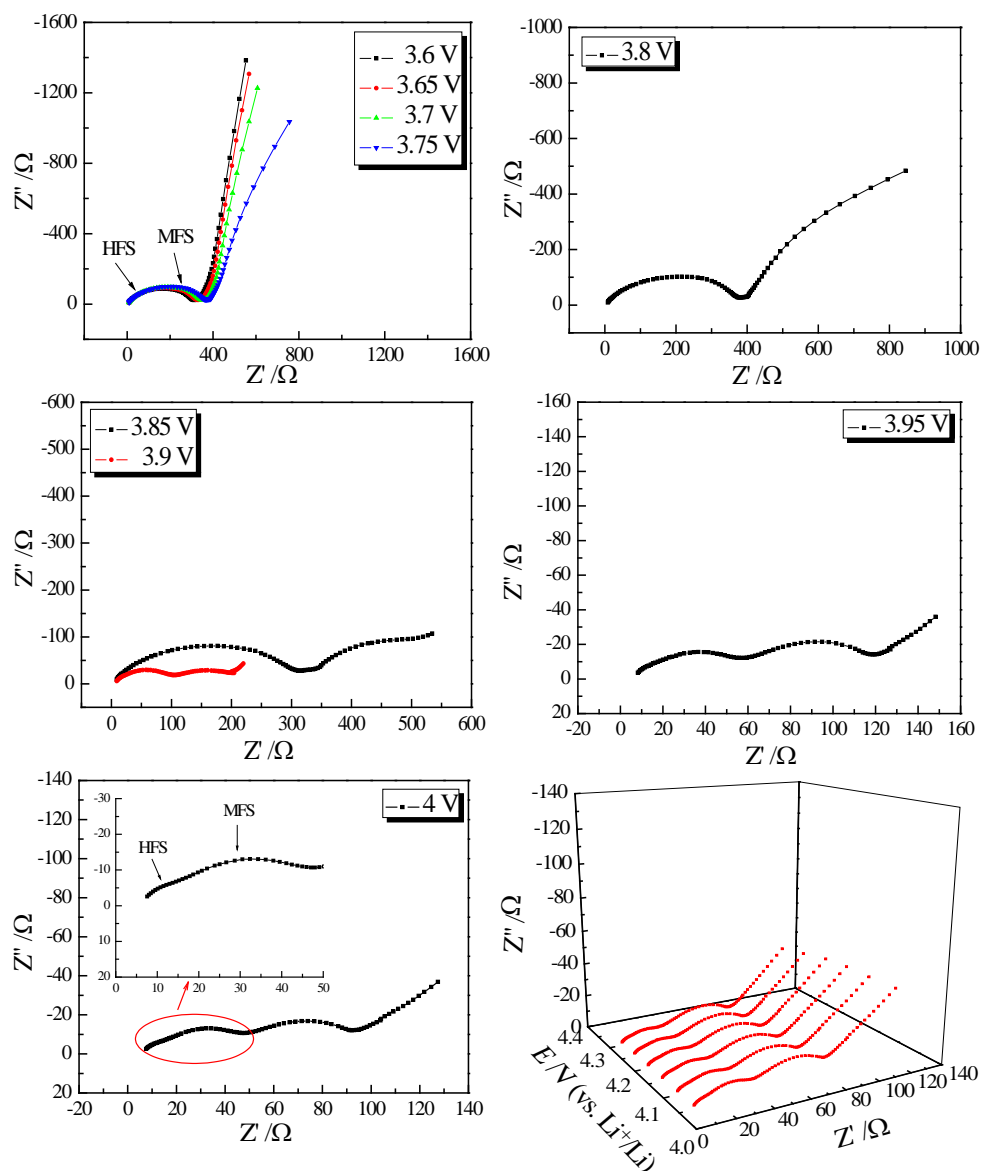


Fig. S2 Nyquist plots of the two-electrode button cell at various potentials from 3.6 to 4.3 V during the first delithiation process.

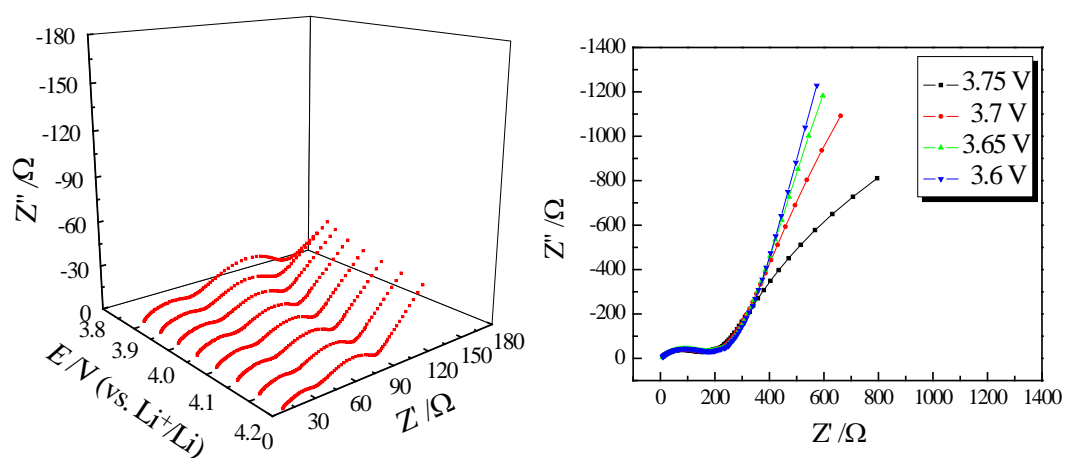


Fig. S3 Nyquist plots of the two-electrode button cell at various potentials from 4.3 to 3.6 V during the first lithiation process.

Note: The common EIS features of LiCoO_2 cathode obtained with two-electrode button cell configuration are similar to those obtained with three-electrode glass cell. However, compared to three-electrode glass cell (shown in Figure 4 and 5), the HF and MF semicircle in Nyquist plots obtained with two-electrode button cell could not be well separated, due to the contributions of the lithium anode, while it is negligible in the three-electrode glass cell.

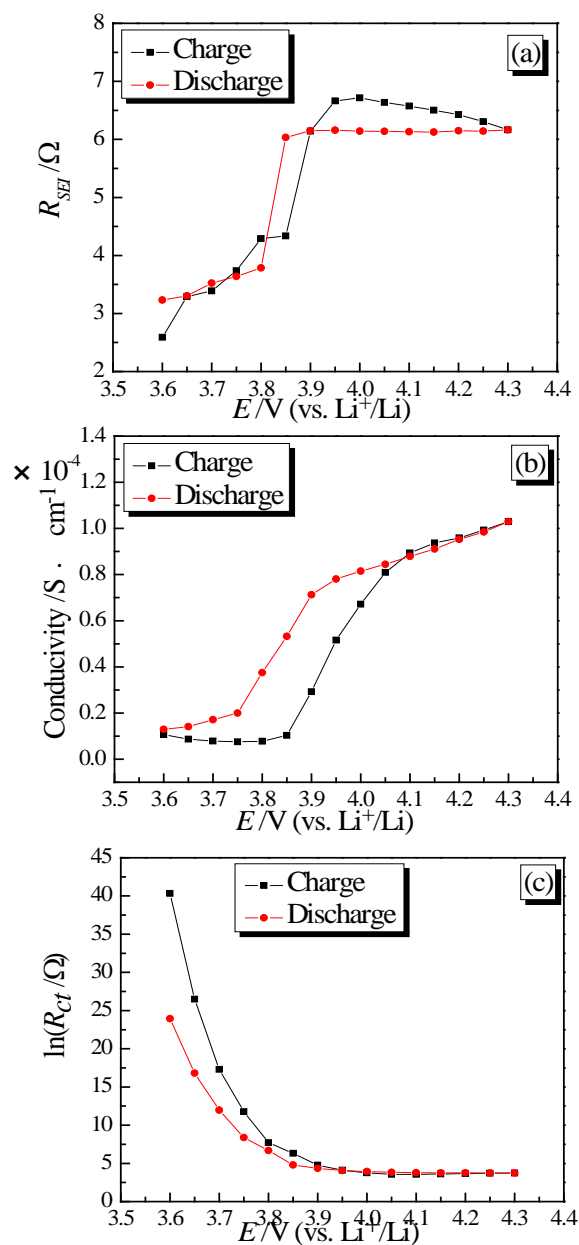


Fig. S4 Variations with electrode potential obtained from fitting the experimental impedance spectra of the LiCoO_2 electrode obtained with the two-electrode button cell during the first charge-discharge cycle. (a) R_{SEI} ; (b) the conductivity derived from R_e ; (c) the logarithm of R_{ct} .

Note: Variations of R_{SEI} against the electrode polarization potential obtained with two-electrode button cell is different from the results acquired with the three-electrode glass cell (shown in Figure 8) due to the contributions of the lithium anode, while it is negligible in the three-electrode class cell. Variations of the electronic conductivity and $\ln R_{\text{ct}}$ against electrode polarization potential obtained with two-electrode button cell during the first charge process are similar to that obtained with three-electrode class cell (shown in Figure 10 and 13). As a consequence, electrochemical impedance experiments could be conducted in a three-electrode glass cell with Li foils as both auxiliary and reference electrodes.

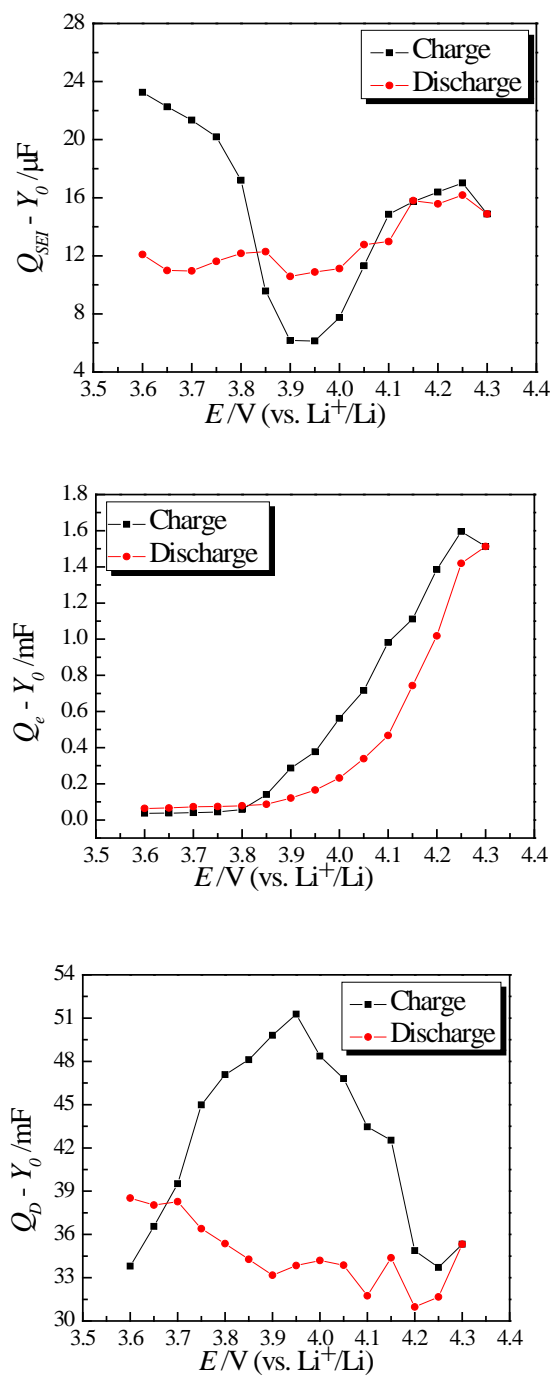


Fig. S5 Variations of capacitance values obtained from fitting the experimental impedance spectra of the LiCoO_2 electrode during the first charge-discharge cycle.
Note: The capacitance values of SEI film are in micro Farads, and the capacitance of the double layer and the associated capacitance used to characterize the electronic properties of the material are in mF.

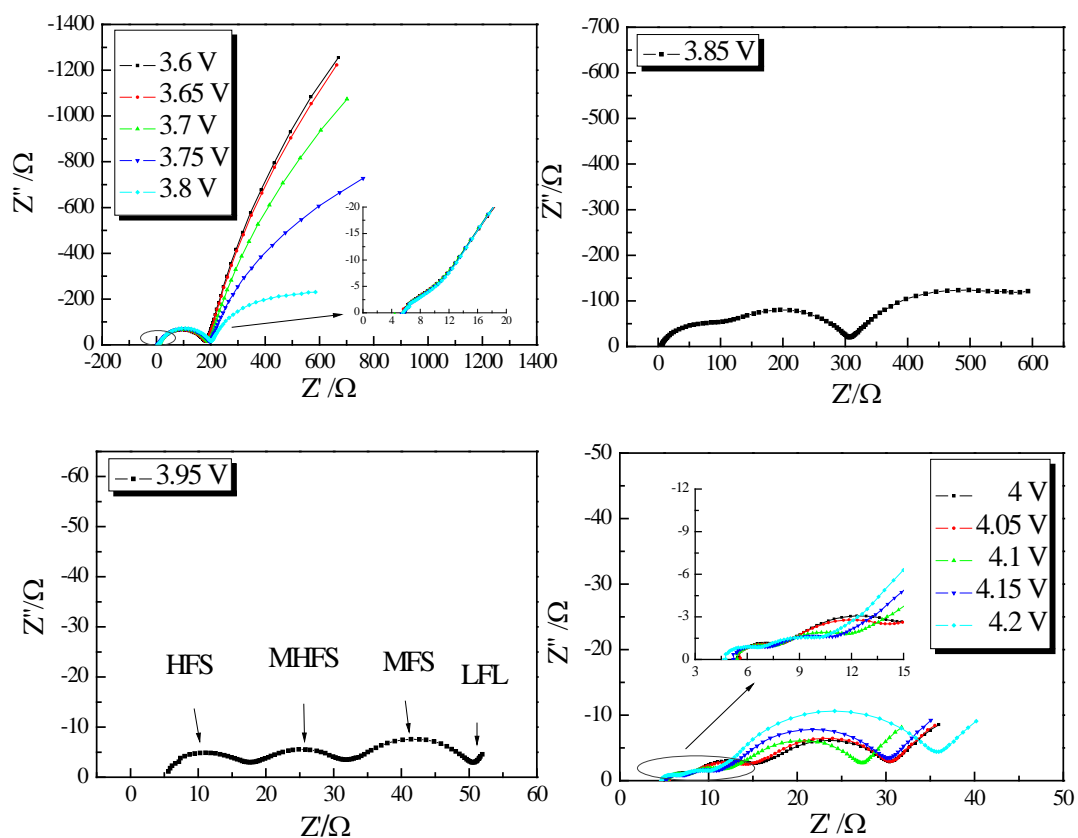


Fig. S6 Nyquist plots of LiCoO_2 electrode obtained with two-electrode button cell at different potentials in the charge process after the 10th cycle.

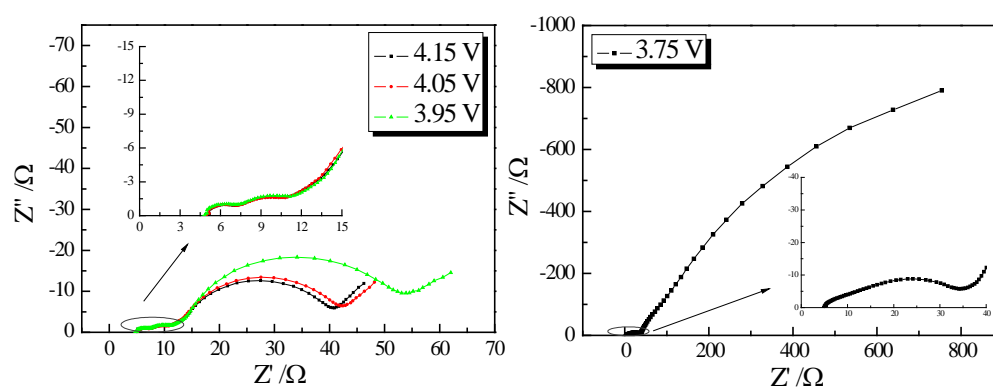


Fig. S7 Nyquist plots of LiCoO₂ electrode obtained with two-electrode button cell at different potentials in the discharge process after the 10th cycle.

Note: The common EIS features of LiCoO₂ cathode obtained with two-electrode button cell after 10th cycle is similar to that recorded with two-electrode button cell at the first charge-discharge process. However, compared to Nyquist plots obtained with two-electrode button cell at the first charge-discharge process (shown in Fig. S2 and S3), the HF and MF semicircle in Nyquist plots acquired with two-electrode button cell could be well separated.

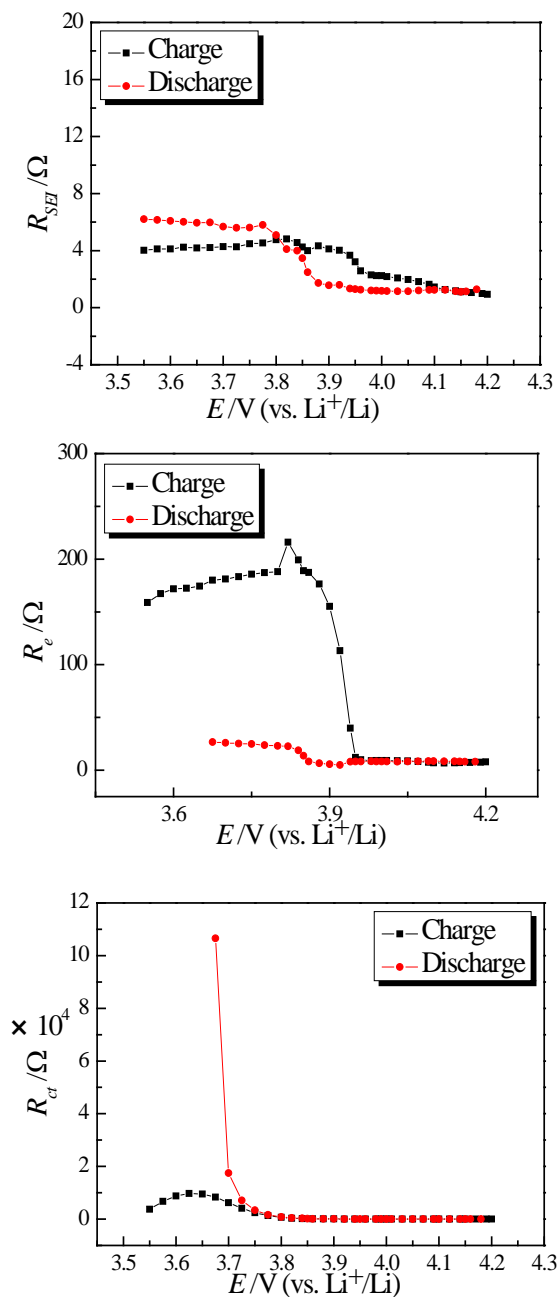


Fig. S8 Variations of R_{SEI} , R_e , R_{ct} with electrode polarization potentials obtained from fitting the experimental impedance spectra of the LiCoO_2 electrode obtained with two-electrode button cell.

Note: Variations of R_{SEI} with the electrode polarization potential obtained with two-electrode button cell after 10th cycle is different from the results acquired with two-electrode button cell at the first charge-discharge process (shown in Fig. S4), due to the formation of the stable SEI film after 10th cycles. Variations of the R_e and $\ln R_{ct}$ against electrode polarization potential obtained with two-electrode button cell after the 10th cycle are similar to that obtained with two-electrode button cell at the first charge-discharge process (shown in Fig. S4).